UDC 537.226.86.681.327.634

Development of Shear-Mode Piezoelectric Microactuator for Precise Head Positioning

●Shinji Koganezawa ●Takeyori Hara

(Manuscript received September 7, 2001)

We have developed a novel piezoelectric micro-actuator for dual-stage actuator systems in magnetic disk drives. This microactuator is based on the shear deformation of piezoelectric elements and drives the head suspension assembly. The actuator is suitable for thin devices and is easily manufactured because of its simple stack configuration.
We installed the microactuator in one of Fujitsu's 3.5-inch commercial drives to evaluate the servo system of a dual-stage actuator. The dual-stage actuator system achieved a non-repeatable position error (NRPE) 3σ of 0.036 μm. The dual-stage servo system reduced the NRPE by 35% compared with the conventional single actuator system, even in HDDs with a high rotational speed of 10 000 rpm.

1. Introduction

Over the last several years, the areal density of magnetic disk drives has increased by 100% every year. Based on this trend, the track density is expected to increase at an annual rate of 40%. In 3.5-inch high-performance hard disk drives (HDDs), the rotational speed of the spindle motor has reached 10 000 rpm and is expected to go even higher. This high rotational speed causes a large windage disturbance and disk flutter, which are serious obstacles to increasing the track density of hard disk drives. To achieve a higher track density, we will need to increase the servo bandwidth.

For the single actuator system, the servo bandwidth is limited by the mechanical resonances of the carriage, coil, and ball bearing pivot. Some types of microactuators have been proposed as possible ways to attain a wider servo bandwidth. Current research on microactuator design may be divided into three types: driving a head suspension assembly,[1)-6)] driving a slider,[7)-9)] and driving a head element.[10),11)] Because head suspension driving microactuators are easy to manufacture, they are expected to be used in HDDs in the near future in spite of their poor mechanical characteristics compared with the slider and head element driving types. Generally, the mechanical characteristics improve as the microactuator is positioned closer to the head. Therefore, the MEMS (Micro-Electro-Mechanical Systems)-based microactuator is expected to be used in the future to achieve a very high track density.

We have developed a piezoelectric microactuator for dual-stage actuator systems that uses the shear mode of piezoelectric elements to drive the head suspension assembly.[4),5)] This paper describes the structure of our shear-mode piezoelectric microactuator and the positioning accuracy of a dual-stage servo system installed in a 3.5-inch high-performance commercial HDD.

2. Piezoelectric actuator types

Our objective was to design a microactuator from piezoelectric elements that has a small and simple structure. For magnetic disk drives, so far,

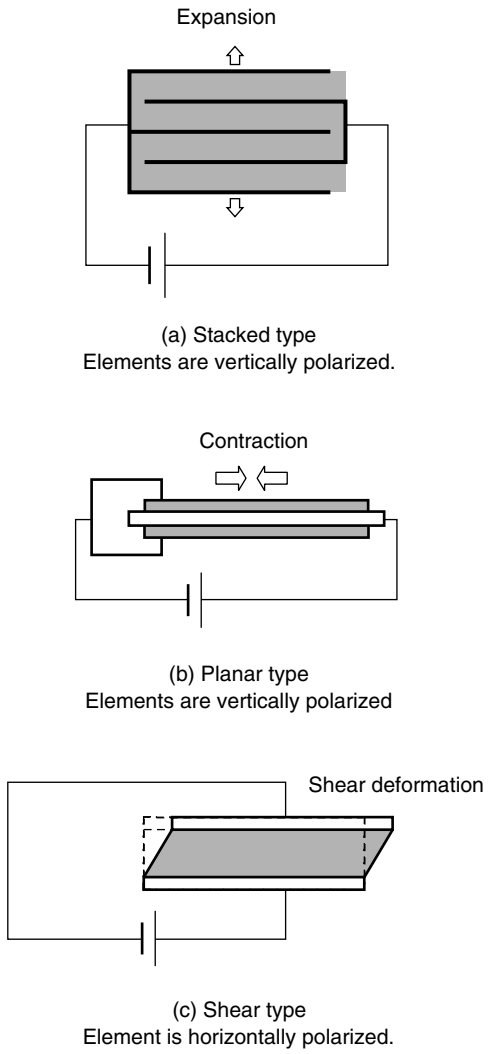

Figure 1
Piezoelectric actuators.

the use of stacked-type and planar-type actuators has been proposed.

Stacked-type piezoelectric actuators (**Figure 1 (a)**) are well known and are commonly used in various fields.[1] They are made by stacking piezoelectric elements on top of each other. When a voltage is applied to both sides of the elements, they expand as shown in the figure. One problem with these actuators is that their complicated structure makes them difficult to assemble. Furthermore, their relative thickness makes them unsuitable for use in thin devices.

The planar-type actuator[2] has a sandwich structure like the bimorph actuator shown in **Figure 1 (b)**. When a voltage is applied to the outside faces of the elements, both elements contract as shown in the figure. This kind of actuator is suitable for thin structures, but its structure is too complicated for head mounting blocks. Another problem is that the force transfer loss is large, because the middle-layer stainless steel sheet to which the piezoelectric elements are bonded prevents the elements from deforming, but if the stainless steel sheet is not used, the fragile piezoelectric elements are easily damaged.

The novel actuator we developed exploits the shear deformation of piezoelectric elements (**Figure 1 (c)**). Here, the piezoelectric element is horizontally polarized. When a voltage is applied to the faces of the element, it becomes sheared. The displacement of the element is estimated by:

$$L = n\,\mathbf{d}_{15}\,V, \qquad (1)$$

where L is the element displacement, n is the number of layers, V is the applied voltage, and $\mathbf{d}_{15}$ is the shear mode piezoelectric constant.

The displacement depends on the shear mode piezoelectric constant and the number of layers and is independent of the dimensions of the element. The piezoelectric element, therefore, can be designed to be small and thin providing it is not thinner than the thickness required by the coercive electric field. Therefore, this actuator is suitable for thin structures. Another advantage of our piezoelectric microactuator is that it has a high shock resistance (see Section 4 for details).

3. Microactuator structure and design

3.1 Structure

Our shear mode piezoelectric microactuator is shown in **Figure 2**. The actuator is comprised of a stator plate, a head mounting block, and a head suspension with a 30% pico-slider (Pico-CAPS).[12] The head suspension is spot-welded onto the microactuator. The piezoelectric elements are polarized in opposition to each other and glued to

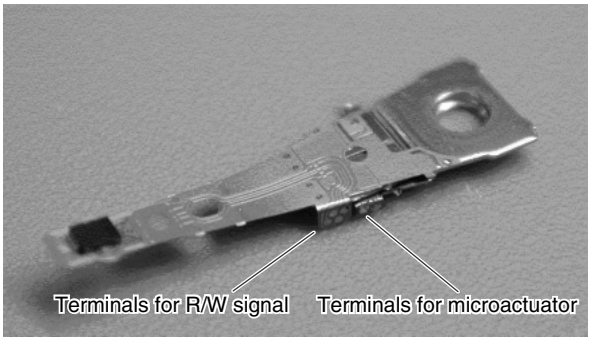

(a) With head suspension

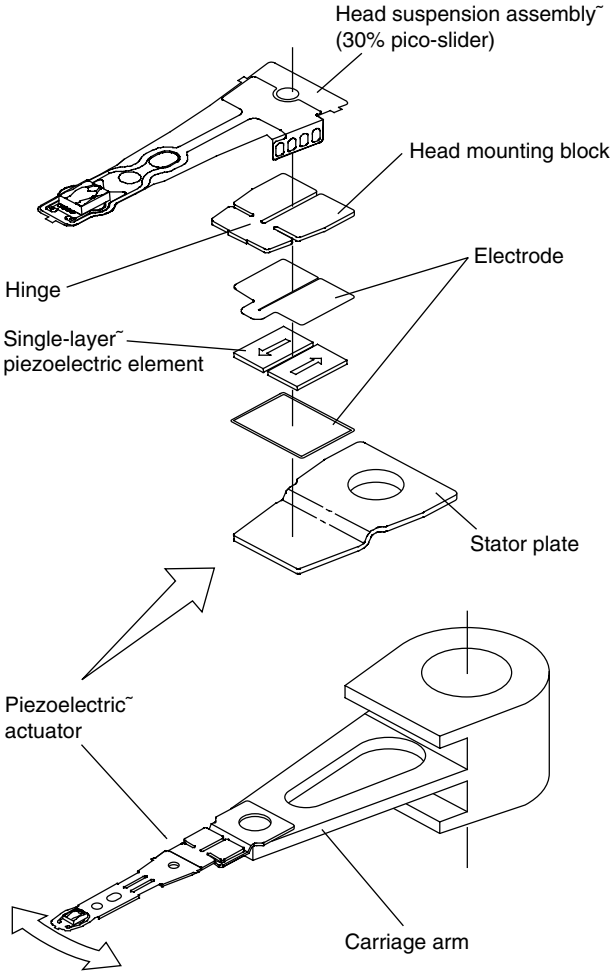

(b) Schematic view of microactuator

Figure 2
Piezoelectric microactuator.

the electrodes. They become sheared in opposite directions to each other when a voltage is applied, which causes the head suspension assembly to swing.

As shown in Figure 2 (b), the microactuator has a hinge structure that amplifies the displacement of the piezoelectric elements. The microactuator assembly has two bonding areas that are connected by a flexible printed circuit. One is for the read/write signal lines, and the other is for the two power lines for driving the microactuator. The head suspension is electrically grounded, and the microactuator's leads are electrically isolated from the head suspension so that the control voltage of the microactuator does not affect the head signal.

Table 1
Specifications of microactuator.

Mass˜ (with head suspension)˜	62 mg˜
Stroke˜	0.5 µm (±30V)˜
Resonant frequency˜	9 kHz˜
Capacitance˜	650 pF˜
Shock resistance	> 950 G, 1 ms half-sine

3.2 Actuator design

We used single-layer piezoelectric elements in order to simplify the manufacturing process. The piezoelectric elements were made of a PZT material which has a $\mathbf{d_{15}}$ constant of 8.45×10^{-10} m/V. The element can generate a displacement of ±25 nm with ±30 V applied. The hinge structure was designed to amplify the displacement of the piezoelectric elements by about 20 times. Therefore, we estimate a displacement of about 1 $\mu m_{p\text{-}p}$ at the head.

The element is 2.2 mm long, 1.3 mm wide, and 0.15 mm thick.

We designed the microactuator to have a small mass of 62 mg so that the resonances of the carriage arm are not excited when the microactuator is driven. Its characteristics are shown in **Table 1**.

The stress in the hinge structure was estimated by FEM (Finite Element Method) analysis. The maximum stress occurs in the notches and equals ±8.4 MPa for a ±0.5 µm head stroke. This

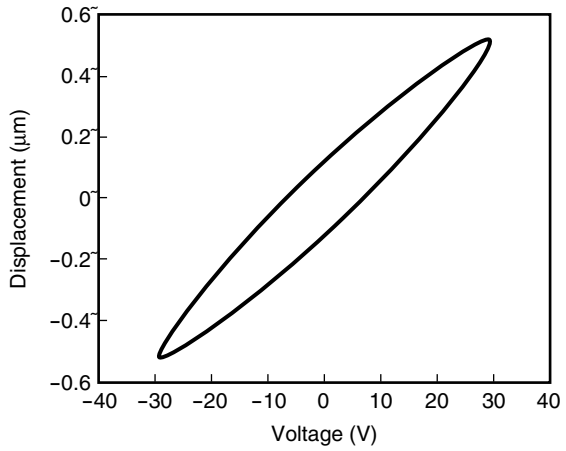

Figure 3
Displacement vs. applled voltage.

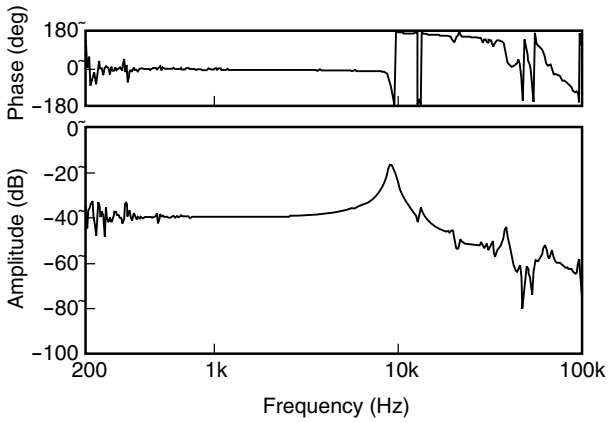

Figure 4
Compllance frequency response of the microactuator.

is less than 5% of the fatigue limit of stainless steel (172 MPa). Thus, repeated stress can be ignored.

4. Mechanical characteristics

4.1 Mechanical response

Figure 3 shows a Lissajous plot of a ±30 V, 1.1 kHz driving signal and the corresponding head displacement. The range of movement at ±30 V is ±0.5 μm. The hysteresis observed in the figure causes the phase lag in the compliance frequency response. Although this is not a fatal fault, it can be a factor that decreases the control performance.

The microactuator's compliance frequency response is shown in **Figure 4**. The microactuator has a high resonant frequency of 9 kHz. The peak

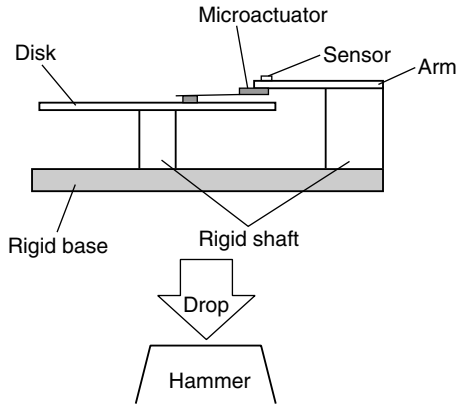

Figure 5
Impact tester.

gain at resonance is approximately 20 dB. This resonance is the coupled mode of the head suspension assembly and the microactuator. The torsion mode of the head-mounting block appears at 20 kHz. These resonant frequencies are high enough for this device to be used as a tracking actuator for magnetic disk drives.

4.2 Shock resistance

Microactuators are required to have high shock resistance so they can be handled easily. We evaluated the microactuator's shock resistance using an impact tester (**Figure 5**). The microactuator and a disk are attached to a rigid base. The assembly was dropped on a hammer, and the acceleration was measured using an accelerometer attached to the tip of the arm. To evaluate the collision damage of the microactuator, we measured and compared its frequency response before and after the impact. We submitted the microactuator to a 1 ms half-sine acceleration of 950 G five times (950 G is the maximum value the tester can generate). We found that the microactuator's frequency response was unchanged by the impact and concluded that the actuator's shock resistance is better than 950 G.

5. Prototype hard disk drive with piezoelectric microactuator

We installed the piezoelectric microactuator in a Fujitsu 3.5-inch commercial drive having a

high rotational speed of 10 025 rpm. This drive uses 3-inch magnetic disks, which reduces the power loss due to windage and also reduces the tracking error caused by disk vibration. The sampling frequency of the prototype HDD was 20 kHz.

The specifications of the prototype drive are shown in **Table 2**.

Figure 6 shows a photograph of the prototype HDD. The microactuator driver IC, which has voltage amplifiers and a DC/DC converter, is indicated on the printed circuit board. The DC/DC converter produces ±18 V from 12 V using a charge pump to supply positive and negative high voltages to the amplifiers. The differential amplifier applies a voltage of ±30 V to the microactuator. In our design, the microactuator's leads are electrically isolated from the head suspension. Therefore, we can use a differential drive amplifier and reduce the supply voltage of the amplifiers.

Table 2
Specifications of prototype hard disk drive.

TPI (tracks per inch)˜	13 500˜
BPI (bits per inch)˜	275 000˜
Rotational speed of spindle motor˜	10 025 rpm˜
Disk diameter˜	3.3-inch˜
Number of disks˜	3˜
Sampling frequency	20.05 kHz

We put resistances in series between the amplifiers and the microactuator. The microactuator is electrically capacitive, so the combination of the microactuator and the series resistances formed an analog low-pass filter. We set the cut-off frequency of the low-pass filter at 8 kHz to eliminate any high frequency component in the microactuator's driving voltage.

6. Servo system of dual-stage actuator

6.1 Servo system

The block diagram of the dual-stage actua-

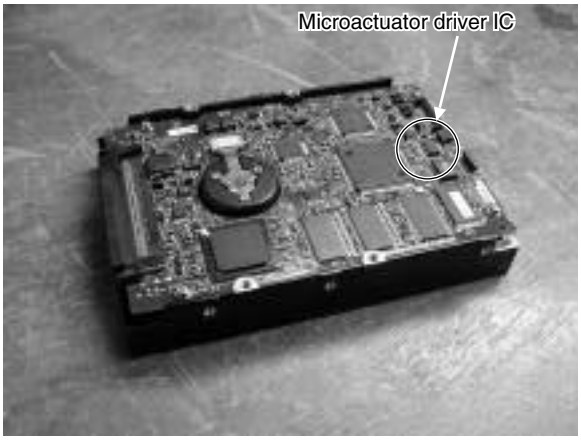

Figure 6
Prototype hard disk drive installed with new microactuators.

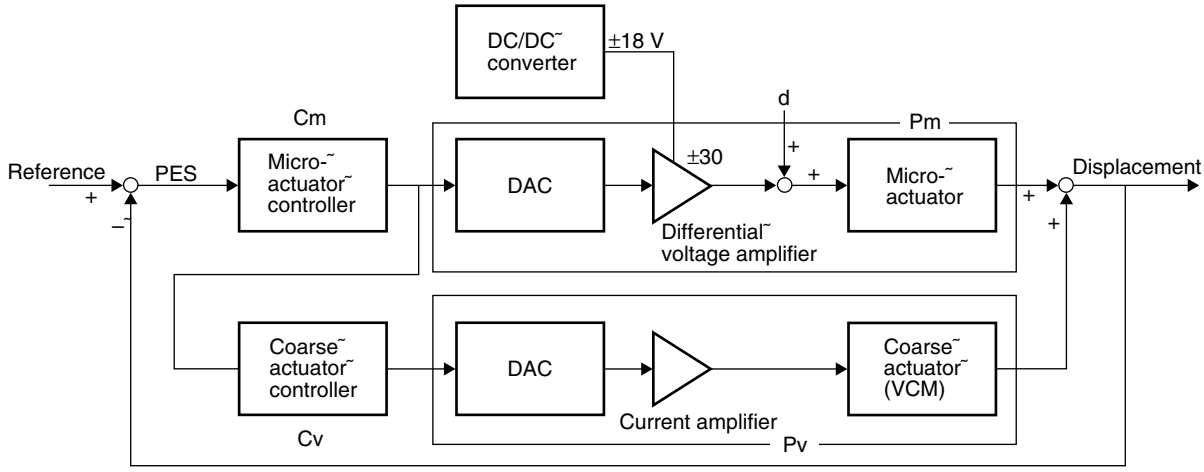

Figure 7
Block diagram of dual-stage actuator system.

tor servo system used in our experiments is shown in **Figure 7**. In this servo system, the microactuator follows the position errors, while the coarse actuator follows the estimated relative displacement between the microactuator and coarse actuator.[5)]

To evaluate the effect of the dual-stage actuator on positioning accuracy, we compared the position error signal (PES) of the dual-stage actuator system with that of a single actuator. We designed the single-actuator controller to have a high crossover frequency of 1 kHz.

The sensitivity function of the single actuator and the approximate sensitivity function of the dual-stage actuator are shown in **Figure 8**. Because the open-loop characteristics could not be measured directly in the dual-stage actuator system, we measured an approximate sensitivity function: the transfer function to the PES from disturbance *d*, which is added to the control voltage. This transfer function is given by:

$$\frac{PES}{d} = \frac{\mathrm{Pm}}{1 + \mathrm{Cm}\,(\mathrm{Pm} + \mathrm{CvPv})} \qquad (2)$$

where Pm and Pv are transfer functions of the microactuator and the voice coil motor (VCM), respectively, and Cm and Cv are their controllers. In the frequency region where the microactuator's compliance gain is flat (< 3 kHz), the sensitivity function is given by:

$$S' \approx \frac{PES}{d \cdot k} \qquad (3)$$

where *k* is the displacement constant of the microactuator (displacement per unit voltage). Figure 8 shows that up to about 2 kHz the dual-stage actuator system can reduce the positioning error better than the single actuator. We calculated the open-loop 0 dB crossover frequency of the dual-stage actuator system from both the S' characteristics and the measured Pm, and obtained a value of approximately 2 kHz.

6.2 PES evaluation

The PES waveforms of the single and dual-stage actuators are shown in **Figure 9**, and the power spectra are shown in **Figure 10**. According to the power spectra, the low-frequency component of the PES was effectively suppressed by the dual-stage actuator system. The high-

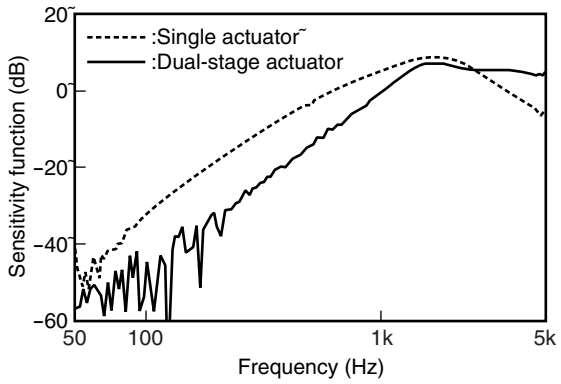

Figure 8
Sensitivity function.

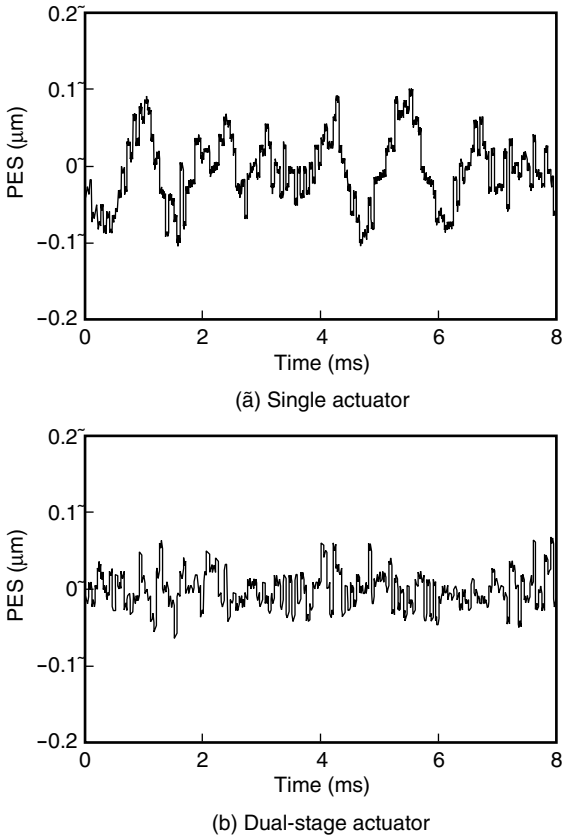

Figure 9
PES waveforms.

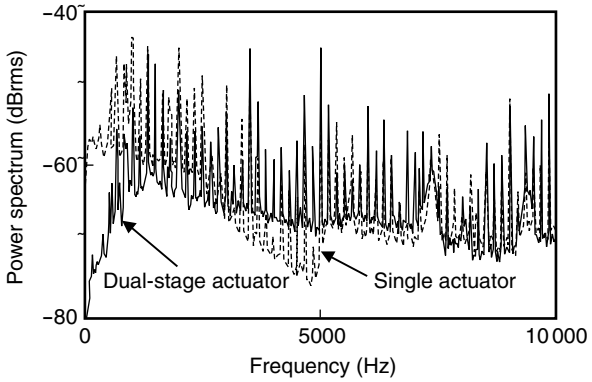

Figure 10
Power spectra of PES.

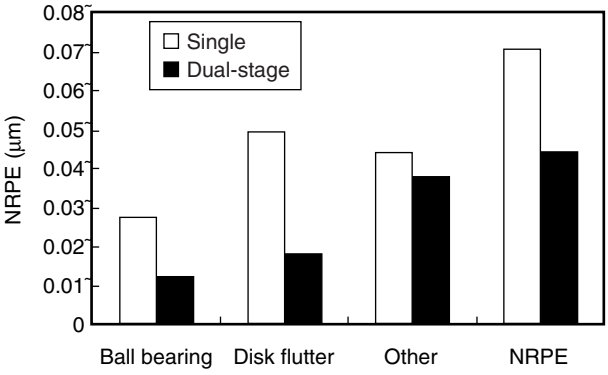

Figure 11
PES components as calculated from the power spectra.

frequency vibration, however, remained. The peak at approximately 9 kHz is the microactuator's dominant resonant frequency, and the peak at 7.5 kHz is the vibration of the carriage arm. These resonances were excited by the wind caused by the disk's rotation rather than by the microactuator's control voltage or VCM's current.

Figure 11 shows the components of the PES as calculated from the power spectra. The ball bearing vibration and disk vibration were reduced by 56% and 59%, respectively. However, other factors, for example, the windage disturbance, noise, and arm resonance, were not reduced much. The resonances at 7.5 and 9 kHz decreased the reduction ratio of the non-repeatable position error (NRPE) in the case of the dual-stage actuator.

The positioning accuracies of both actuator systems are compared in **Table 3**. The 3σ (three

Table 3
Positioning accuracies of single and dual-stage actuators.

(a) NRPE (3σ)

Zone	Single actuator (VCM)	Dual-stage actuator	Reduction
Outer	0.073 µm	0.046 µm	36%
Center	0.073 µm	0.047 µm	35%
Inner	0.059 µm	0.036 µm	39%

(b) TPE (3σ)

Zone	Single actuator (VCM)	Dual-stage actuator	Reduction
Outer	0.089 µm	0.069 µm	23%
Center	0.091 µm	0.071 µm	22%
Inner	0.093 µm	0.074 µm	21%

times the standard deviation) values of NRPE were within 0.047 µm, and the 3σ values of the total position error (TPE) were within 0.074 µm for the dual-stage actuator, even in HDDs with a high rotational speed of 10 000 rpm. The effect of the dual-stage actuator on reducing NRPE was about 35% in every zone. The reduction rate of the TPE was approximately 22%. The reduction rate of the repeatable run-out (RRO) was only 10%, because we used the RRO compensator in the VCM controller of both actuator systems to reduce the RRO. The low-frequency RRO was compressed enough by the RRO compensator, even in the single actuator system. Therefore, the effect on the TPE was small in this experiment.

7. Conclusion

We have developed a piezoelectric microactuator that uses the shear deformation of piezoelectric elements. It has a high resonant frequency of 9 kHz. The range of movement is ±0.5 µm at ±30 V. We installed the microactuator in a Fujitsu 3.5-inch high-performance hard disk drive having a high rotational speed of 10 025 rpm. We achieved a servo bandwidth of approximately 2 kHz with a dual-stage actuator system. The dual-stage actuator system had a 35% lower non-repeatable position error than the single actuator system and a 22% lower TPE. In the dual-stage actuator, the

3σ values of the NRPE were within 0.047 µm and the 3σ values of the TPE were within 0.074 µm, even in HDDs with a high rotational speed of 10 krpm.

References

1) K. Mori, T. Munemoto, H. Otsuki, Y. Yamaguchi, and K. Akagi: A dual-stage magnetic disk drive actuator using a piezoelectric device for a high track density. *IEEE Trans. Magn.*, **27**, 6, p.5298-5300 (1991).
2) T. Imamura, S. Hasegawa, K. Takaishi, and Y. Mizoshita: Piezoelectric Microactuator Compensating for Off-Track Errors in Magnetic Disk Drives. *ASME Adv. Info. Storage Syst.*, p.119-126 (1993).
3) S. Koganezawa, K. Takaishi, Y. Mizoshita, Y. Uematsu, T. Yamada, S. Hasegawa, and T. Ueno: A Flexural Piggyback Milli-Actuator for over 5 Gbit/in^2. Density Magnetic Recording. *IEEE Trans. Magn.*, **32**, 5, p.3908-3910 (1996).
4) S. Koganezawa, Y. Uematsu, T. Yamada, H. Nakano, J. Inoue, and T. Suzuki: Shear Mode Piezoelectric Microactuator for Magnetic Disk Drives. *IEEE Trans. Magn.*, **34**, 4, p.1910-1912 (1998).
5) S. Koganezawa, Y. Uematsu, T. Yamada, H. Nakano, J. Inoue, and T. Suzuki: Dual-Stage Actuator System for Magnetic Disk Drives Using a Shear Mode Piezoelectric Microactuator. *IEEE Trans. Magn.*, **35**, 2, p.988-992 (1999).
6) R. B. Evans, J. S. Griesbach, and W. C. Messner: Piezoelectric Microactuator for Dual Stage Control. *IEEE Trans. Magn.*, **35**, 2, p.977-982 (1999).
7) Y. Soeno, S. Ichikawa, T. Tsuna, Y. Sato, and I. Sato: Piezoelectric piggyback microactuator for hard disk drive. *IEEE Trans. Magn.*, **35**, 2, p.983-987 (1999).
8) L. -S. Fan, H. H. Ottesen, T. C. Reiley, and R. W. Wood: Magnetic Recording Head Positioning at Very High Track Densities Using a Microactuator-Based, Two-Stage Servo System. *IEEE Trans. on Industrial Electronics.*, **42**, 3, p.222-233 (1995).
9) W. Tang, V. Temesvary, R. Miller, A. Desai, Y. C. Tai, and D. K. Miu: Silicon Micromachined Electromagnetic Microactuators for Rigid Disk Drives. *IEEE Trans. Magn.*, **31**, 6, p.2964-2966 (1995).
10) T. Imamura, T. Koshikawa, and M. Katayama: Transverse Mode Electrostatic Microactuator for MEMS-Based HDD Slider. *IEEE, MEMS*, p.216-221 (1996).
11) S. Nakamura, K. Suzuki, M. Ataka, and H. Fujita: An electrostatic microactuator for a magnetic head tracking system of hard disk drives. Proc. of International Conference on Micromechatronics for Information and Precision Equipment, Tokyo, p.58-63 (1997).
12) T. Ohwe, T. Watanabe, S. Yoneoka, Y. Mizoshita: A New Integrated Suspension for Pico-Sliders (PICO-CAPS). *IEEE Trans. Magn.*, **32**, 5, p.3648-3650 (1996).

Shinji Koganezawa received the B.S. and M.S. degrees in Mechanical Engineering from Tokyo Institute of Technology, Tokyo, Japan in 1989 and 1991, respectively. He joined the research staff at Fujitsu Laboratories Ltd. in 1991 and moved to Fujitsu Ltd. in 1993. His primary research interest is the actuator system for precise positioning, especially dual-stage actuator systems for magnetic disk drives. He is a member of the Japan Society of Mechanical Engineers (JSME). He received the Outstanding Presentation Award from the JSME Information, Intelligence, and Precision Equipment Division in 1996.

Takeyori Hara received the B.E. degree in Mechanical Engineering from the University of Tokyo, Tokyo, Japan in 1993. He joined Fujitsu Ltd., Kawasaki, Japan in 1993, where he has been engaged in design and development of servo controllers for hard disk drives. From 1996 to 1998, he was a Visiting Industrial Fellow at the Mechanical Engineering Department, University of California, Berkeley. He is a member of the Japan Society of Mechanical Engineers (JSME).